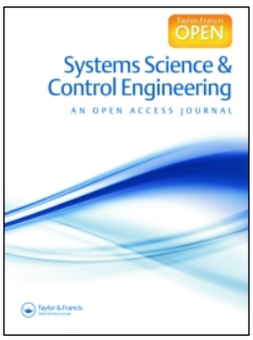

Systems Science & Control Engineering

An Open Access Journal

ISSN: (Print) 2164-2583 (Online) Journal homepage: http://www.tandfonline.com/loi/tssc20

Design and implementation of an innovative electronic magnetic gearing motor

Xiao Guo, Nabeel Shirazee, Guo-Ping Liu & Jonathan Williams

To cite this article: Xiao Guo, Nabeel Shirazee, Guo-Ping Liu & Jonathan Williams (2017) Design and implementation of an innovative electronic magnetic gearing motor, Systems Science & Control Engineering, 5:1, 9-15, DOI: 10.1080/21642583.2016.1262800

To link to this article: https://doi.org/10.1080/21642583.2016.1262800

Published online: 07 Dec 2016.

SYSTEMS SCIENCE & CONTROL ENGINEERING: AN OPEN ACCESS JOURNAL, 2017
VOL. 5, NO. 1, 9–15
https://doi.org/10.1080/21642583.2016.1262800

Taylor & Francis
Taylor & Francis Group

Design and implementation of an innovative electronic magnetic gearing motor

Xiao Guo[a], Nabeel Shirazee[b], Guo-Ping Liu[a] and Jonathan Williams[a]

[a]Faculty of Advanced Technology, University of South Wales, Pontypridd, UK; [b]Electronica Products Limited, Cardiff, UK

ABSTRACT
This paper presents an innovative electronic magnetic geared (EMG) motor. The motor is designed and tested. This electronic EMG motor assembles parallel, serial or hybrid connections of stator windings into gears to accommodate the different speed and torque demands in the drive cycle. The objective of EMG is to increase the maximum speed and maximum torque range of the motor. A 1.5 kW prototype EMG motor was built up and tested on a test rig. The test results prove that the theory of EMG is correct. It will have a large positive impact on the energy efficiency of electric vehicles.

ARTICLE HISTORY
Received 17 October 2016
Accepted 16 November 2016

KEYWORDS
Component; hybrid electric vehicle; PMSM motor; energy saving

1. Introduction

Low carbon vehicle technology with renewable energy has been a very popular research topic during the past decade. Many researchers believe electric vehicles (EVs) will be the best solution from tight oil supplies in the near future. EVs are normally driven by electric motors that are powered by energy storage units (ESUs), such as a battery, a supercapacitor or a hydrogen fuel cell. However, no matter what kind of ESU is chosen, it provides the same electric power. Due to this limited on-board power source, EVs provide a very limited driving range compared with traditional internal combustion engine vehicles.

Many different kinds of motors have been tested on EVs, with the most commonly used one being a permanent magnet DC (PMDC) motor. It has the advantages of higher efficiency and a lower susceptibility to mechanical wear. With the modern control methods such as vector control or direct torque control, a DC motor gives a much better dynamic performance on EVs.

Figure 1 shows a typical speed–torque graph of a PMDC motor. In this graph, the DC motor has a constant torque below the base speed and a constant power beyond the base speed.

In this way, there comes a trade-off problem between starting torque and constant power range. From a vehicle dynamic point of view, when the vehicle starts up, accelerates or climbs up a hill, the output torque from the motor should be as high as possible to enhance the car performance. In a practical design, motor rated torque is limited by rated current of the inverter and its own current limit. With the same manufacturing cost of the motor, a higher rated torque design will make the speed range of the constant power shorter. In this way, the maximum speed of the motor becomes smaller and the cruising distance of the vehicle is also reduced. When a large torque is provided, a bigger current will drain from the battery to support the motor, which will generate a lot of heat. Either from the point of view of energy efficiency or from vehicle safety, a higher current is not good for EVs.

Many solutions have been introduced to solve this trade-off problem between starting torque and constant power range. The most common solution is a continuously variable transmission (CVT). With a CVT, the torque can be multiplied at the start and the maximum speed is also extended, as shown in Figure 2. The problem for a CVT is that the efficiency is normally about half of a fixed ratio gear transmission due to the friction effects. The system efficiency is quite low (45–80%) compared with the fixed ratio gear transmission system (90–95%) (Chen & Cheng 2005; Tsai, Chou, & Chu 2001). From an energy efficiency point of view, a CVT is not a good solution for long-term use in EVs.

Researchers have started to think about new ways to build up motors in order to overcome this speed–torque problem. Huang and Chang (1997) proposed an electrical two-speed propulsion system by switching induction motor windings between a serial connection for starting an EV and a parallel connection for normal speed operation. Yang, Liu, Wang, Kuo, and Hsu (2007) made use of

CONTACT Xiao Guo guoxiao@gmail.com

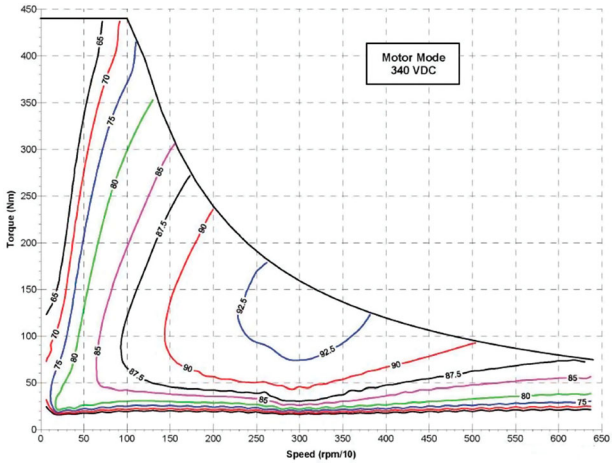

Figure 1. Speed–torque curves for a DC motor.

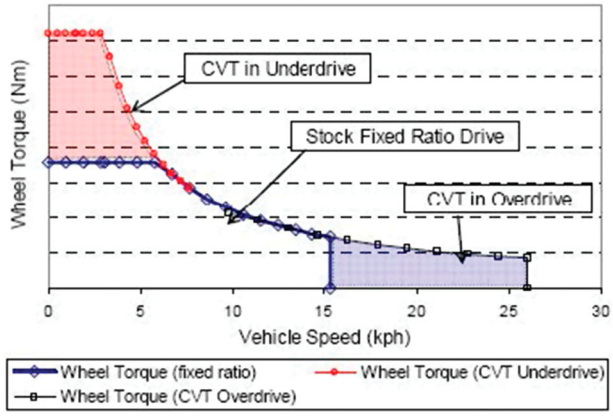

Figure 2. Speed–torque curve of a DC motor with CVT.

a winding changeable axial flux DC motor with a group of supercapacitors. The supercapacitors are connected in serial or parallel with the motor at different gears. This system requires a lot of insulated gate bipolar transistor (IGBT) switches and diodes, which are very bulky and expensive. Moreover, the axial flux design is not suitable for high dynamic performance use in EVs. Also with these previous researches, the motor efficiency issue was not considered at gear switching.

This paper presents an innovative design of radial flux PMDC motor with electronic magnetic gearing (EMG) on windings. This motor with gear shifting increases the rated torque, which improves the whole system's performance. Gear shifting technique also increases the range of constant power and extends the maximum speed of the motor. With all these features, compared with traditional DC motor, the EMG motor has a wider application range and better energy efficiency.

2. Design of EMG

A normal radial flux three-phase brushless DC motor can be simplified as shown in Figure 3. The stator has

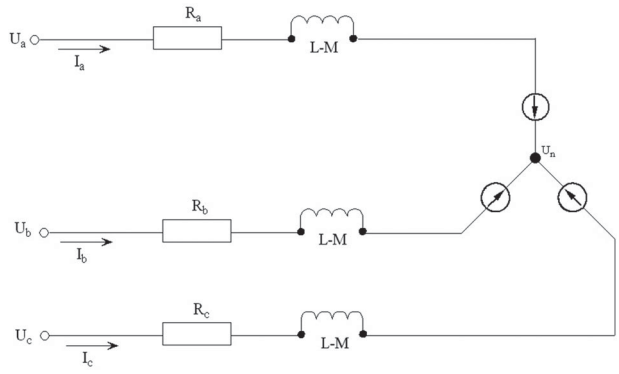

Figure 3. Electric circuit of a brushless DC motor.

windings all around and the rotor rotates in the centre. The rotor is made of permanent magnetic material.

In a normal PMDC motor circuit, the theoretical equation can be expressed as follows:

$$\begin{bmatrix} u_A \\ u_B \\ u_C \end{bmatrix} = \begin{bmatrix} R_s & 0 & 0 \\ 0 & R_s & 0 \\ 0 & 0 & R_s \end{bmatrix} \begin{bmatrix} i_A \\ i_B \\ i_C \end{bmatrix} + p \begin{bmatrix} L_A & M_{AB} & M_{AC} \\ M_{BA} & L_B & M_{BC} \\ M_{CA} & M_{CB} & L_C \end{bmatrix} \begin{bmatrix} i_A \\ i_B \\ i_C \end{bmatrix} + p \begin{bmatrix} \psi_r^A \\ \psi_r^B \\ \psi_r^C \end{bmatrix}, \quad (1)$$

where u_A, u_B and u_C are the voltages of the three-phase windings. In each phase, i_A, i_B and i_C are currents of the three-phase windings and in each phase; ψ_r^A, ψ_r^B and ψ_r^C are the permanent magnetic flux linkage projection components on each windings; p is the differential operator; L_A, L_B and L_C are the inductances on the windings and M_{AB}, M_{AC}, M_{BA}, M_{BC}, M_{CA} and M_{CB} are the mutual inductances between the three windings.

After Clarke transforms and Park transforms, the PMDC's voltages in the d–q system can be expressed as follows:

$$\begin{bmatrix} u_d \\ u_q \end{bmatrix} = R_s \begin{bmatrix} i_d \\ i_q \end{bmatrix} + \begin{bmatrix} L_d & 0 \\ 0 & L_q \end{bmatrix} p \begin{bmatrix} i_d \\ i_q \end{bmatrix} + \omega \begin{bmatrix} 0 & -L_q \\ L_d & 0 \end{bmatrix} \begin{bmatrix} i_d \\ i_q \end{bmatrix} + \omega \begin{bmatrix} \psi_f \\ 0 \end{bmatrix}. \quad (2)$$

The flux linkage in the d–q system is

$$\begin{bmatrix} \psi_d \\ \psi_q \end{bmatrix} = \begin{bmatrix} L_d & 0 \\ 0 & L_q \end{bmatrix} \begin{bmatrix} i_d \\ i_q \end{bmatrix} + \begin{bmatrix} \psi_f \\ 0 \end{bmatrix}. \quad (3)$$

And the torque in the d–q system is

$$T_{em} = \psi_s i_s = p_n[\psi_f i_q + (L_d - L_q) i_d i_q], \quad (4)$$

where p_n is the number of pole pairs, ψ_f is the permanent magnetic flux linkage, L_d and L_q are the inductances on d–q axis and i_d and i_q are the currents on the d–q system.

Definition of the stator current's space vector is i_s, and it is in the same phase as stator's flux linkage vector ψ_S. The angle between stator's flux linkage and permanent magnetic flux linkage is β; so current in the d–q system is

$$\begin{aligned} i_d &= i_s \cos\beta, \\ i_q &= i_s \sin\beta. \end{aligned} \tag{5}$$

Taking Equation (5) into Equation (4) gives

$$\begin{aligned} T_{em} &= p_n[\psi_d i_q - \psi_q i_d] = p_n \psi_f i_s \sin\beta \\ &\quad + \frac{1}{2} p_n (L_d - L_q) i_s^2 \sin 2\beta. \end{aligned} \tag{6}$$

Equation (6) shows that the permanent magnet synchronous motor (PMSM) torque includes two parts, one is the electromagnetic torque generated by magnetic field, and the other one is the resistance torque generated by the salience effect.

In the steady state of a PMSM, ignoring the effect from the resistance, from Equations (2) and (3), we can get the motor speed (Morimoto, Sanada, & Takeda, 1996):

$$\begin{aligned} u_d &= -\omega L_q i_q, \\ u_q &= \omega L_d i_d + \omega \psi_f. \end{aligned} \tag{7}$$

So the speed of motor can be expressed as

$$\omega = u / \sqrt{(L_q i_q)^2 + (L_d i_d + \psi_f)^2}. \tag{8}$$

In the control loop, the voltage and current are limited by the rated voltage and current of the IGBT inverter. Definition of $u_{\max}$ is the maximum voltage of the inverter and $i_{\max}$ is the maximum current of the inverter. The speed of the motor under maximum voltage is therefore

$$\begin{aligned} \omega &= \frac{u_{\max}}{\sqrt{(L_q i_q)^2 + (L_d i_d + \psi_f)^2}}, \\ &= \frac{u_{\max}}{\sqrt{(L_q i_s \cos\beta)^2 + (\psi_f - L_d i_s \sin\beta)^2}}. \end{aligned} \tag{9}$$

In order to examine the demagnetizing effects of the permanent magnet due to the d-axis armature reaction, the demagnetizing coefficient ξ is defined as the ratio of the d-axis armature reaction flux to the permanent magnet flux linkage ('Expansion of operating limits,' 1989).

$$\xi = \frac{L_d i_s}{\psi_f}. \tag{10}$$

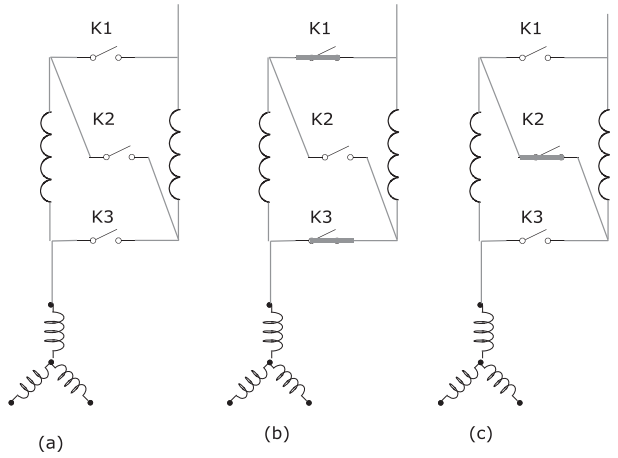

Figure 4. Different on/off settings of switches in one phase of an EMG motor.

Definition of the saliency coefficient ρ is the ratio of L_d and L_q (Morimoto, Takeda, Hirasa, & Taniguchi, 1990):

$$\rho = \frac{L_d}{L_q}. \tag{11}$$

Substituting Equations (10) and (11) into Equation (9), the base speed of a PMSM is therefore

$$\omega = \frac{u_{\max}}{\psi_f \sqrt{(\rho\xi \cos\beta)^2 + (1 - \xi \sin\beta)^2}}. \tag{12}$$

As an example, phase A of a motor's stator will be analysed as a sample phase. If all windings of phase A are simplified into two turns, and these two turns of windings connect all IGBT switches in the following way, it will make a simple circuit, as shown in Figure 4.

In Figure 4(a), all switches are shut. There is no current passing through; so there is no torque generated. In Figure 4(b), switches K1 and K3 are on and K2 is off. The windings are connected in parallel. In Figure 4(c), switch K2 is on, switches K1 and K3 are off. The windings are connected in series.

Figure 4 is a simplified winding model. In practical use, there are more than two turns of winding in each phase. Assuming each phase has n turns of windings, each winding's resistance is R and inductance is L, as shown in Figure 5. In one connection 'H', the number of windings in the parallel connection is m, the number of windings in series connection is $n-m$. If m is 1, all windings are connected in series. If m equals n, all windings are connected in parallel, if m is between 1 and n, we define it as a hybrid connection. In the following equations, subscripts 's' and 'r' denote stator and rotor quantities. Superscript 'p', 's' and 'h' represent full parallel connection, full series connections and hybrid connection.

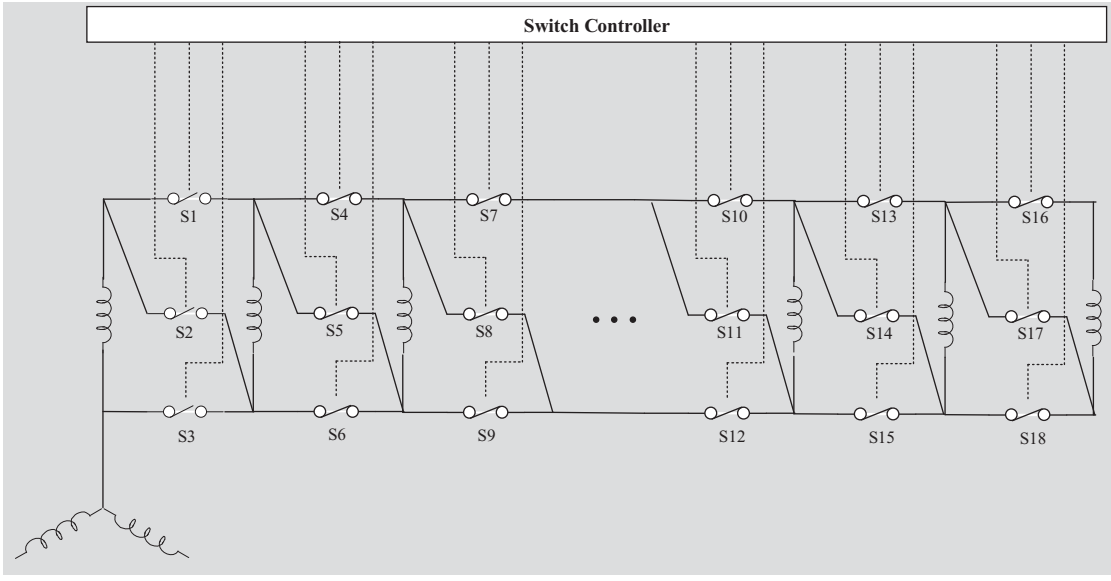

Figure 5. Hybrid connection of an EMG motor in one phase.

Take phase A's simplified windings as an example, if the windings change from full series to full parallel, the changes of inductance and flux linkage will be

$$\begin{aligned} L_d^s &= 4L_d^p, \\ L_q^s &= 4L_q^p, \\ \psi_f^s &= 2\psi_f^p. \end{aligned} \tag{13}$$

Substituting Equation (13) into Equations (6) and (12) gives,

$$T_{em}^s = 2T_{em}^p + (L_d^p - L_q^p) i_{\max}^2 \sin 2(\beta^p + 90), \tag{14}$$

and

$$\omega_{\max}^s / \omega_{\max}^p = \frac{\sqrt{[\rho\xi^p \sin(\beta^p + 90)]^2 + [1 + \xi^p \cos(\beta^p + 90)]^2}}{2\sqrt{[2\rho\xi^p \sin(\beta^p + 90)]^2 + [1 + 2\xi^p \cos(\beta^p + 90)]^2}}. \tag{15}$$

In an EMG motor, the saliency coefficient ρ is 1, where $L_d = L_q$ and $\beta = 0$, so that the equations can be simplified to

$$T_{em}^s = 2T_{em}^p, \tag{16}$$

$$\omega_{\max}^s / \omega_{\max}^p = \frac{\sqrt{1 + (\xi^p)^2}}{2\sqrt{1 + 4(\xi^p)^2}}. \tag{17}$$

From the above equations we can see, after windings change from series to parallel, that the maximum torque output is reduced to half, and the base speed increased.

3. Simulation of the EMG system

A PMSM closed-loop control system is built in Matlab/Simulink. The PMSM specs in the simulation are based on a real 200 watts PMSM. The specs are in Table 1.

In the simulation, the reference speed of the motor is 150 rad/s, which is 1432 rpm. The initial load is 4 Nm and reduces to 2 Nm after 0.2 s. The windings change from series to parallel at 0.2 s. The simulation result is as follows.

The output torque is shown in Figure 6.

The motor output speed is shown in Figure 7.

The stator currents are shown in Figure 8.

The simulation results show that the motor gives good dynamic responses with the speed and torque demands. The output torque reduces to half after windings are changed from series to parallel; meanwhile the input current stays the same. The simulation results prove that Equations (16) and (17) are correct. In an EMG motor,

Table 1. PMDC motor specifications.

Rated power	200 W
Rotor moment of inertia	0.0008 kg m^2
Rated torque	3.5 Nm
Rated voltage	310 V
Rated current	1.5 A
Stator's resistance	2.875 Ω
Rated inductive reactance	0.0085H
Rated speed	1500 rpm
Number of poles	4

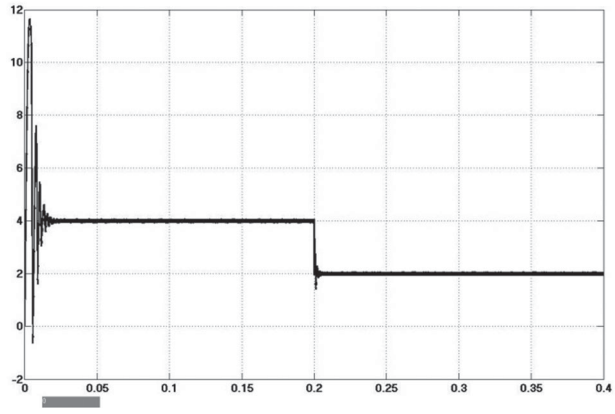

Figure 6. Torque output of EMG motor.

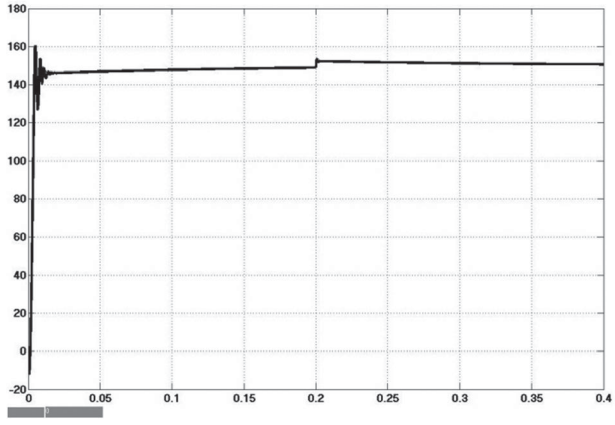

Figure 7. Speed output of an EMG motor.

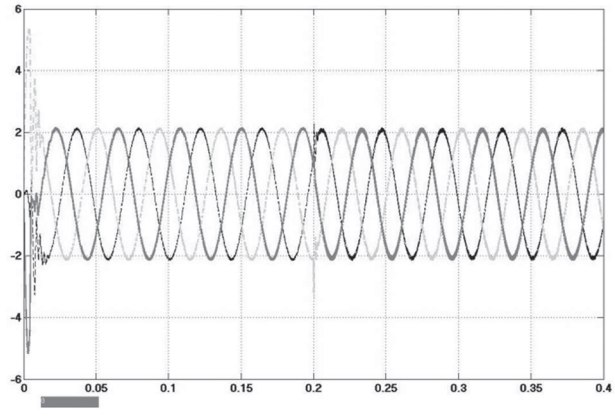

Figure 8. Stator currents of an EMG motor.

series connection can provide more torque with the same input current than with a parallel connection.

4. EMG motor test rig and configuration

Followed by the variable winding change theory, a prototype EMG motor and a system test rig was built up for a 1.5 kW EMG motor. The motor was driven by a full

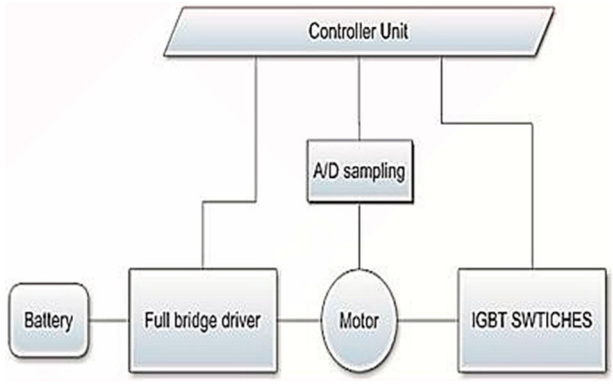

Figure 9. Connection of the EMG motor test rig.

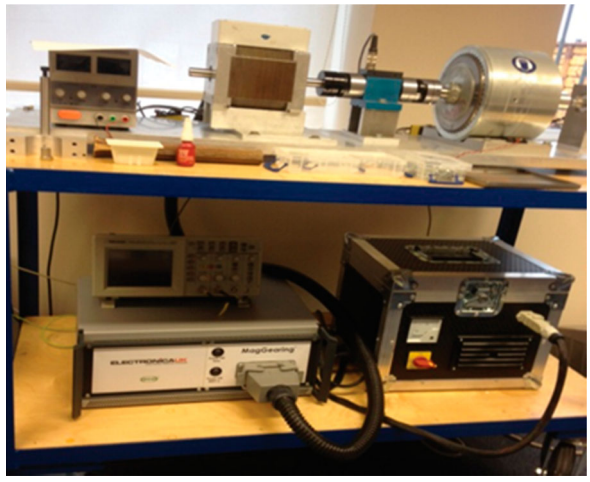

Figure 10. Test rig of the 1.5 kW EMG motor.

bridge driver, which was connected to a lithium-ion battery. The speed and torque demands could be either read from a drive cycle profile or adjust manually. The IGBT switches' ON/OFF signals were generated from the controller and sent to the switches; these signals followed a pre-setup rule for different motor gears. Figure 9 shows the connection of all these components.

The test rig of the 1.5 kW prototype EMG motor is shown in Figure 10. In the practical test, a DC motor was used as a load to simulate different resistances of the load.

The EMG motor in this test was set with three gears. This meant that the windings had three different connections. The IGBT switches' on/off profiles of different winding connections were pre-load to the controller. Gear 1 was set up as the full parallel gear, two shift points were set up for gear switching; the points are where the lines cross each other. The gears could be shifted both manually and automatically.

Figure 11 is the speed–torque test result of the 1.5 kW EMG motor with three gears. This test result shows that gear 3's base speed is 1/4 of gear 1's base speed, while gear 3's maximum torque is 4 times gear 1's maximum

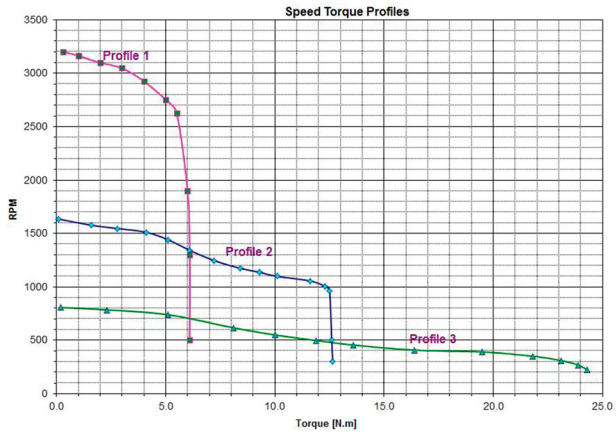

Figure 11. Test result of three gears in 1.5 kW EMG motor.

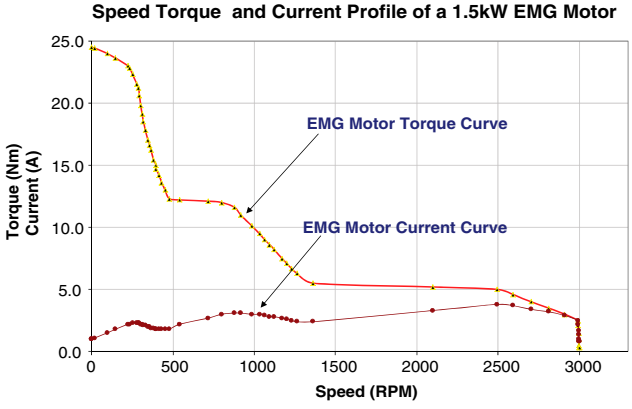

Figure 12. Speed–torque and current curve of a 1.5 kW EMG motor.

torque. Gear 2's base speed is 1/2 of gear 1's base speed, while gear 2's maximum torque is 2 times that of gear 1's maximum torque. These results show that Equations (16)–(19) are correctly applied.

In practical work, the 1.5 kW EMG motor will work with a speed–torque curve as shown in Figure 12. The rated torques of different gears switched at switching points. The test results show that the current is almost at the same level in all gears. In the EMG motor, for different speed torque demands, it can always give a better energy efficiency output. Compared with the traditional PMSM, the EMG motor covers a much larger working speed range as well.

5. Summary and conclusions

In this research, an innovative radial flux EMG motor has been successfully analysed, simulated, built and tested on a test rig. Compared with traditional motors, this motor increased the start torque and extended the operational range of constant power. It will improve the efficiency of the whole EV system. The controller is properly built for gear selection by the demand of speed/torque and the gear efficiency. Theoretical analysis and experimental results of the 1.5 kW EMG motor test have verified that a satisfactory performance is achieved by using the proposed method.

An EV with EMG system can provide higher start torque and higher cruise speed. This can give better sprint performance and better climb performance for an EV. With the system controller, the EMG system can always find the optimize point to give better torque output, which can save energy and increase driving range. Traditional method used in EV to increase the start torque is a gearbox or a fixed ratio transmission. With EMG system, there is no need for a gearbox, which reduces weight, saves room and no more gearbox maintenance. For some special industrial areas, where both high speed and high torque are needed, EMG motor will have great potential in these particular applications.

More research may be necessary for smooth gear changing by field weakening. In the practical test, when the gear changed at the shift points, the system had step vibrations. A proper field weakening can make the system speed–torque curve smoother and reduce the shock at gear changing points. Advanced intelligent measure method and control method such as fuzzy logic control can improve the controller's dynamic performance (Luo & Wang, 2016a, 2016b). Also, due to technical limitations, the hybrid connection could only be set when part of the windings was fully parallel and the remainder series connected. A mixed connection should give more speed torque curves, which will cover more working points.

Disclosure statement

No potential conflict of interest was reported by the authors.

References

Chen, C.-H., & Cheng, M.-Y. (2005). *Study on a wide speed range integrated electrical transmission system*. Proceedings of 6th IEEE international conference on power electronics and drive systems (pp. 781–786). Kuala Lumpur, Malaysia.

Expansion of operating limits for permanent magnet motor by optimum flux-weakening. (1989). Industry Applications Society Annual Meeting, Conference Record of the 1989 IEEE.

Huang, H., & Chang, L. (1997, May 4–7). *Tests of electrical-two-speed propulsion by induction motor winding switching for electric vehicles*. IEEE 47th Vehicular Technology conference (Vol. 3, pp. 1907–1911), Phoenix, Arizona.

Luo, Y., & Wang, Z. (2016a). H∞ control for 2-D fuzzy systems with interval time-varying delays and missing measurements. *IEEE Transactions on Cybernetics*, (99), 1–12.

Luo, Y., & Wang, Z. (2016b). Robust H-infinity filtering for a class of two-dimensional uncertain fuzzy systems with randomly

occurring mixed delays. *IEEE Transactions on Fuzzy Systems*, (99), 1.

Morimoto, S., Sanada, M., & Takeda, Y. (1996). Inverter-driven synchronous motors for constant power. *IEEE Industry Applications Magazine*, *2*(6), 18–24.

Morimoto, S., Takeda, Y., Hirasa, T., & Taniguchi, K. (1990). Expansion of operating limits for permanent magnet motor by current vector control considering inverter capacity. *IEEE Transactions on Industry Applications*, *26*(5), 866–871.

Tsai, M. C., Chou, M. C., & Chu, C. L. (2001). *Control of a variable winding brushless motor with the application in electric scooters.* Proceedings of IEMDC'01 (pp. 922–925). Massachussets, USA.

Yang, Y.-P., Liu, J.-J., Wang, T.-J., Kuo, K.-C., & Hsu, P.-E. (2007). An electric gearshift with ultracapacitors for the power train of an electric vehicle with a directly driven wheel motor. *IEEE Transactions on Vehicular Technology*, *56*(5), 2421–2431.